Effects of pH control by acid addition at the aqueous processing of cathodes for lithium ion batteries

Werner Bauer [a, *], Fatih A. Çetinel [a, b], Marcus Müller [a], Ulrike Kaufmann [a]

[a] Karlsruhe Institute of Technology Institute for Applied Materials – Energy Storage Systems (IAM-ESS), P.O. Box 3640, 76021, Karlsruhe, Germany
[b] BASF SE, Carl-Bosch-Strasse 38, 67056, Ludwigshafen am Rhein, Germany

Keywords:
NMC
Aqueous processing
Acetic acid
Adhesion
Aging

A B S T R A C T

The replacement of organic solvent-based electrode manufacturing by a water-based process offers the chance for a significant reduction of the manufacturing costs. However, the interaction of cathode materials with water changes their storage properties and causes massive problems for electrode manufacturing and cell properties. Due to a Li^+/H^+ exchange reaction, the pH of the aqueous slurry is increased so that a corrosive attack of the aluminum foil takes place. The reduction of the pH value by the addition of an acid is a practical measure to prevent corrosion, but has also negative effects on slurry rheology, or electrode conductivity and adhesion. These consequences are shown in an exemplary way for the addition of acetic acid. As especially the adhesion strength is influenced, this effect is investigated in detail for various acids. Best electrode properties are not found in the stable region of the aluminum foil, but at a higher pH of 9–10. Acetic acid treated cells show high capacities at their begin-of-life, but undergo stronger degradation than samples without acid addition.

1. Introduction

Manufacturing processes for lithium ion batteries primarily use non-aqueous solvents for the production of cathode coatings [1]. The most prevalent solvent is N-methyl-pyrrolidone (NMP) [2]. It is established because of its good solubility for polyvinylidene fluoride (PVDF), which has advantages when used as binder for cathodes or anodes due to its high electrochemical stability and good adhesion strength. However, replacing the organic solvent-based with a water-based process would be desirable as it is more sustainable and allows a significant reduction of the manufacturing costs. This is not only due to the lower cost of water and many water compatible binders [3–6], but also due to reduced invest and operation costs for production plants which result from minor efforts for worker protection and explosion prevention [7]. In addition, disposal of the solvent after the drying process is easier for water as no solvent recovery or thermal post-combustion is required. On the other hand, the substitution of NMP by water is a step which massively interferes with many levels of the production chain, requiring a lot of adjustments in order to ensure at least comparable process and product properties [8–10].

Examples for the additional complexity of the water-based process are a reduced colloidal stability of the slurries which is caused by the existence of hydrogen bonding and strong electrostatic forces [11] and the chemical interaction of electrode components with water. Especially cathode materials tend to react with water causing severe problems for the subsequent processing steps. Due to their metal oxide base, conventional cathode materials form hydroxides when they are in contact with water (Fig. 1) [12]. Additionally, hydroxide formation is caused by a Li^+/H^+ exchange reaction that takes place by the leaching of lithium ions [10,13]. Leached Li^+ ions rapidly react with oxygen or moisture to Li_2O and LiOH, which are subsequently transferred to Li_2CO_3 by dissolved CO_2 [14–16]. During the storage in humid atmosphere, a nanometer thick carbonate layer is formed on the particle surface [17], but when the material is immersed, the hydroxide is dissolved in the water. Consequently, the pH value of the aqueous dispersion significantly increases to the basic range. The resulting pH values depend on the used cathode material, supplementary slurry components and the time of exposure. Reported values can be found in Table 1. It can be deduced from this compilation that a trend to higher pH values exists for high capacity materials. On the anode side, $Li_4Ti_5O_{12}$ (LTO) has a significant impact on the pH value too.

A high pH value is critical for the electrode coating process once

* Corresponding author.
E-mail address: werner.bauer@kit.edu (W. Bauer).

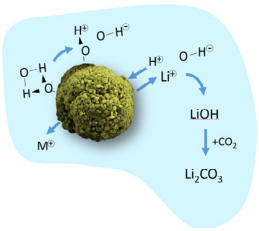

Fig. 1. Reactions of cathode materials in an aqueous environment.

Table 1
Native pH values in aqueous dispersions of electrode materials.

Electrode material	pH	Ref.
$LiFePO_4$ (LFP)	9	[18]
$LiMn_{1.5}Ni_{0.5}O_4$ (LMNO)	10.3	own result
$LiCoO_2$ (LCO)	11.6	[19]
$Li(Ni_{1/3}Mn_{1/3}Co_{1/3})O_2$ (NMC111)	11.7	[20]
$Li(Ni_{0.6}Mn_{0.2}Co_{0.2})O_2$ (NMC622)	12.3	own result
$Li(Ni_{0.8}Co_{0.15}Al_{0.05})O_2$ (NCA)	12.3	[21]
$Li(Ni_{0.8}Mn_{0.1}Co_{0.1})O_2$ (NMC811)	12.4	[22]
$Li(Ni_{0.81}Co_{0.16}Al_{0.03})O_2$	13.1	[20]
$Li_4Ti_5O_{12}$ (LTO)	11.4	[23]

the slurry gets into contact with the aluminum current collector foil. The aluminum surface is protected by an oxide layer which is stable only within the pH range from 4.5 to 8.5 [12]. At higher pH, the oxide layer is dissolved and a corrosive attack of the metal foil takes place. This can lead to the formation of water soluble Al species [24], both general corrosion and pitting of the Al foil [20,25], and to the generation of gas bubbles which are trapped inside the electrode layer [19]. As all of these effects may have detrimental consequences for the electrode properties, various approaches have been developed to overcome this problem. The pH value can be reduced by the addition of an acid, for example by hydrochloric acid [19], formic acid [3,26,27] or phosphoric acid [23,24,27]. Another approaches affect the pH by a pressurized CO_2 gas treatment [21] or by addition of amphoteric oxidic additives [25]. A carbon coating was applied on the aluminum foil in order to protect the metal surface [12,28]. Direct contact of the active materials with water was reduced by a protective coating made from VO_x [29], by metal phosphates [24,27] or a binder shell [24].

In this paper, the slurry modification approach using acids is investigated for NMC111 as a representative cathode material. Acetic acid (HAc) is primarily added in order to reduce the pH of the slurry to moderate values. Acetic acid is of interest, as it is expected to vaporize during the electrode-drying step, leaving less or no residues in the final electrode. Acetic acid is also less hazardous than formic acid. In contrast to other investigations on acid treatment, this paper is particularly focusing on the impact of the pH modification on slurry and electrode processing, since the knowledge of these effects is required for a better understanding of the electrochemical behavior of the electrodes. Special emphasis is placed on the clarification of adhesion aspects. Complementing the HAc experiments by poly acrylic acid (PAA) and other acids allows accentuating the acid specific effects.

2. Experimental

Commercial $LiNi_{1/3}Mn_{1/3}Co_{1/3}O_2$ cathode material (NMC) was delivered by BASF SE, Germany. It has a mean particle size of 8.9 µm and a BET surface of 0.37 m^2/g. For aqueous electrode preparation, the cathode material was mixed with sodium carboxy methylcellulose binder (CMC) from Dow Wolff Cellulosics, Germany (CRT 2000 PA), water-based fluorine acrylic copolymer latex binder (LB) from JSR Corporation, Japan (TRD202A) and carbon black (CB) from Imerys Graphite & Carbon, Switzerland (Super C65) in deionized water. The carbon black has a BET surface of 62 m^2/g and a mean TEM primary particle size of 35 µm. For poly acrylic acid, three variants were used, a short-chained type with 2000 g/mol (PAA-2k) and high-molar mass types with 450,000 g/mol (PAA-450K) and 1,250,000 g/mol (PAA-1.25M).

5 wt% of the NMC powder was dispersed in de-ionized water by a magnetic stirrer for the determination of the lithium leaching process. The concentration of lithium, nickel, manganese and cobalt in the aqueous phase was measured at particular leaching times and pH values by ICP-OES (OPTIMA 4300DV, Perkin-Elmer). For this investigation, the adjustment of the pH was done by addition of 1M HCl.

Mixing of the electrode slurries was performed in a vacuum equipped dissolver (VMA Getzmann, Germany). At first, powdery components NMC and carbon black were added to a premixed aqueous CMC stock solution to get a final solid content of 25 vol%. The acid was admixed immediately after the collection of all powders. Mixing was done at 2000 RPM for 90 min, followed by a 3-min vacuum phase at identical speed for degassing. Finally, the shear sensitive latex binder was added to the slurry by gentle stirring at 500 RPM and vacuum-homogenized for 2 min. The solid components are adjusted to a ratio of NMC:CB:CMC:LB = 100:3:2:3 in the dried cathode. PAA-450K or PAA-1.25M were premixed with water and due to the binder-like behavior of these PAA types, the amount of CMC was reduced by the equal mass.

Electrodes were cast on a 20-µm thick aluminum foil using a roll-to-roll coater (KTF-S, Mathis AG, Switzerland) with knife coating device at a gap of 130 µm and a speed of 0.2 m/min. The electrodes were dried by convection in a first stage at 40 °C air temperature, followed by a second stage at 80 °C. As each stage had a length of 0.9 m, drying was completed in less than 10 min. Compaction of the electrodes was done in a heated calendar at 50 °C to an electrode porosity of 39–43 vol%, and later for the aging tests to 35–38 vol%. The electrodes produced had an NMC loading between 12.2 and 14.4 g/cm^2 (11.7–12.7 g/cm^2 for the aged samples).

Pouch cells with ceramic-coated separator foil (Separion®, Litarion, Germany) and about 20% overbalanced graphite anode (SMG A, Hitachi, Japan) were prepared for electrochemical tests. Electrode size was 50×50 mm^2 for the cathode and 54×54 mm^2 for the anode. Before assembly, all electrodes and separators were dried overnight in a vacuum furnace at 130 °C. The pouch cells were assembled in a dry room at a dew point of below 50 °C. The electrolyte was LP30 (1:1 EC/DMC with 1 M $LiPF_6$) obtained from BASF SE, Germany. After assembly, all cells were stored 20 h at 40 °C to facilitate a homogeneous distribution of the electrolyte within the electrode.

The pH value was measured 10 min after finishing the mixing procedure. Following the pH measurement, the slurry was immediately transferred into the coating device. Rheological tests were carried out using steady state flow measurements in a rheometer (MCR 300, Paar Physica, Austria) with plate-plate geometry (PP50) at a temperature of 25 °C. A reference shear rate of 50 1/s was chosen for comparing the slurry viscosities as this value approximates typical conditions in the coating device.

The electrode resistivity was determined before calendaring. Discs with a diameter of 14 mm were punched out of the electrodes and placed between two polished copper cylinders with a diameter of 14 mm. For better electrical contact, a thin indium foil was additionally placed between the NMC side and the copper cylinder. A pressure of 6.5 kPa was applied on the cylinders while the across-the-electrode resistance was measured by a milliohm meter

(RM3544, Hioki E.E. Corporation, Japan). The impedance of the pouch cells was measured with a battery tester (BT3554, Hioki E.E. Corporation, Japan) at 1 kHz.

Adhesion strength was measured in a universal testing machine (UTS T-10, Zwick, Germany) with in-house developed 90° peel test device, based on DIN EN 28510-1. Electrode stripes (width 17 mm) were fixed on a metal plate by double-sided adhesive tape with the NMC layer facing the tape. The whole stack was pressed with a defined load of 200 kg for 2 s and then fixed with an uncoated end of the aluminum foil at the vertical traverse by a clamp. For the measurement, the force was logged while the traverse is moving at a constant speed of 600 mm/min.

For SEM investigation of the electrode microstructure, cross-sections were prepared by using a triple ion beam cutter system (EM TIC-3X, Leica Microsystems, Germany) with argon as working gas. In case of post-mortem inspections, the cycled cells were opened in an argon-filled glove box and intensively washed with DMC to remove electrolyte residues, followed by a vacuum drying step.

The electrochemical performance was measured in a temperature-controlled room at 23 °C. Voltage limits were set at 3.0 V and 4.2 V. The C-rate was calculated based on the theoretical capacity of the NMC cathode material with graphite anode (155 mAh/g). In a first section, all cells were cycled in galvanostatic mode (constant current, CC). Formation was performed in two cycles at C/20 charging and discharging rate, followed by symmetrical cycles with C/2, 1C, 2C, 3C and again C/2, each rate repeated 10 times and finished by 50 cycles at 1C. For aging tests, cycling was continued with selected cells in constant current-constant voltage mode (CCCV) at 2C charging and 3C discharging rate. After every 100 cycles, the CCCV program was intermitted by a segment of 10 cycles with 1C charging/discharging, enabling a comparison with the capacity of the initial CC section.

3. Results and discussion

3.1. Cation extraction from NMC in aqueous dispersion

Water or humidity leaches cations out of the NMC. Table 2 shows, that the process is dominated by the extraction of lithium. The proton exchange immediately starts when the particles are dispersed in water. A large portion is extracted within the first minute, later the release rate drops substantially. This means that lithium is primarily leached out from the surface, while diffusion from deeper layers takes place much slower. After 30 min, 17.8 mg/l lithium is dissolved in the aqueous phase, corresponding to an amount of 0.46% of the original lithium fraction from the NMC particles. By equating the concentration of the dissolved Li^+ with the concentration with the OH^- concentration in the dispersion, a pOH value of 2.6, respectively a pH of 11.4 is calculated, matching the measured pH value. Assuming that all particles are identical spheres with a diameter of 8.9 µm, after 30 min exposure time, this is equivalent to a delithiated shell with a thickness of 7 nm. This calculation is in good accordance with the results of Zhang [15] who investigated the interaction of NMC with a humid atmosphere by magnetic measurements.

An increase of the proton activity by adding an acid shifts the equilibrium and enhances the exchange coefficient for the lithium ions. At pH 9 and above, other cations are hardly detectable. However, at a pH of 7, also nickel, manganese and cobalt ions can be discovered in significant quantities in solution. This result confirms for this cathode material the outcome of other studies that the active materials are most stable at the native pH [18,27,28,30].

Table 2
Concentration of extracted cations in aqueous NMC suspensionsby ICP-OES. The native pH is 11. Lower pH values are adjusted by addition of 1M HCl.

Elements	Concentration/mg/l (5 wt% NMC in water, T = 21 °C)				
	pH 7, 10 min	pH 9, 10 min	pH 11, 1 min	pH 11, 10 min	pH 11, 30 min
Li	21.9	17.7	14.1	15.4	17.8
Mn	3.4	0	0	0.1	0
Co	3.1	0	0	0.1	0.1
Ni	4.8	0	0	0.1	0.1

3.2. Control of pH by addition of acetic acid

The pH of the slurry depends particularly on the composition and on the mixing time. For the used additives, only the latex binder significantly decreases the pH value by around 0.5 to 1, but the pH values remain above 10. In order to reduce the pH further, acetic acid (HAc) has to be added to the slurry. Even very small additions of HAc have a significant impact on the pH value. An amount of 0.5 wt% of HAc was revealed as being sufficient for attaining the stability zone of alumina below pH 8.5.

The addition of HAc initially has only a minor influence on the viscosity of the slurry (Fig. 2). An effect, which becomes more obvious by the addition of the acid, is the alteration of the surface quality of the dried electrodes. The surface becomes smoother with ongoing reduction of the pH value, which is even visible for the unaided eye. This effect can be explained by the improved comminution of carbon black agglomerates. As-delivered carbon black is strongly agglomerated and must therefore be disintegrated during slurry mixing. As a polyelectrolyte, CMC is not only a binder, but is also able to stabilize the shredded carbon black fragments by electrosteric means [31]. Nevertheless, CMC is less effective as dispersant than acetic acid. Therefore, more carbon black agglomerates are destroyed in the dissolver mixing process.

Beneath a pH value of 9, the viscosity is rising again. Similar results for the pH dependency of the viscosity were published by Li et al. for a $LiCoO_2$ slurry [19]. The viscosity rise was explained by the agglomeration of the active material. However, this is unlikely for our system as neither NMC nor carbon black dispersions show an alteration of the zeta potential in the relevant pH range [32]. A possible explanation can be given by the pH dependency of

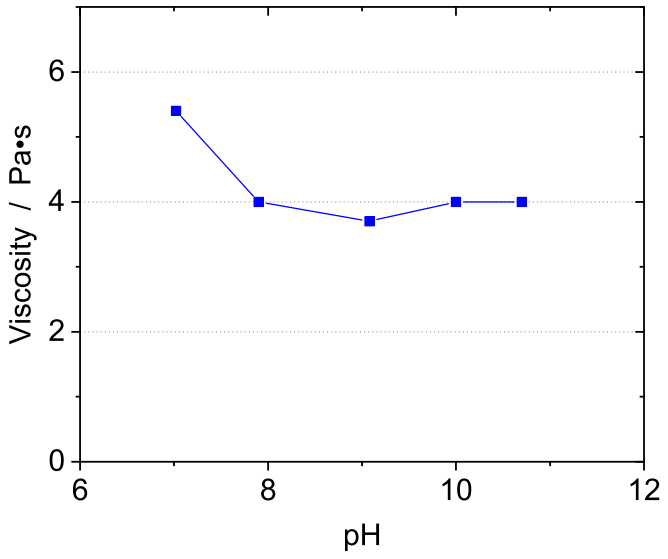

Fig. 2. pH dependence of slurry viscosity with addition of acetic acid (viscosity is determined at a reference shear rate of 50 1/s).

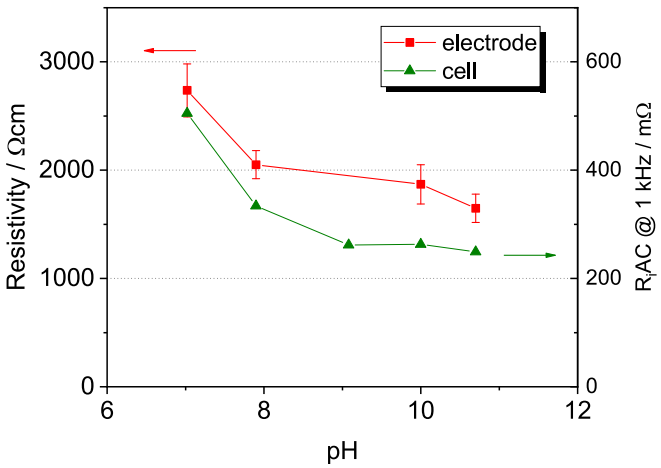

Fig. 3. DC resistivity of uncalendared electrodes and AC cell impedance after addition of acetic acid.

aqueous CMC solutions. The addition of protons causes conformational changes of the polyelectrolyte chains. A less coiled conformation is formed at pH 7, which generates more entanglement of the polymer chains and therefore a higher viscosity [33,34], accompanied by a maximized swelling in the neutral pH region [35]. However, also relevant could be an effect, which is affected by the carbon black. Fig. 3 reveals that the DC resistivity of the electrodes, which is primarily influenced by the arrangement of the carbon black particles, shows a comparable tendency at low pH values like the viscosity. The strong de-agglomeration effect of HAc produces a larger fraction of carbon black fragments, but these parts do not necessarily improve the electrical conductivity of the electrode. In fact, they seem to form an increased number of isolated particles, which are homogeneously deposited on the surface of the NMC after drying, having no electrical connection to other CB particles [36]. In addition, an increased number of small particles in the slurry assists to unfold the polymer coils of the CMC, causing extended bridging between particles and more entanglement between the chains, which will increase the viscosity.

Such isolated CB fragments can be discovered at pH 7 in SEM micrographs quite well (Fig. 4). Nevertheless, this should be seen more as a hint than a proof for the hypothesis as the micrographs only show a limited segment of the carbon distribution with a lack of statistical confidence.

3.3. *Investigation of the impact on adhesion strength*

Another effect, which is caused by the addition of HAc, is a drastic change of the adhesion strength of the electrode coating on the aluminum foil (Fig. 5). Since fewer gas bubbles are formed at the interphase, the electrode has more contact area and the adhesive strength is initially improved by a minor reduction of the pH. However, below a pH of 10, the adhesion drops so extremely that even low stresses cause delamination of the electrode.

Better understanding of the impact of acids on the adhesion strength will be obtained by repeating the acetic acid experiments with other acids. By that, it becomes obvious that this effect is not

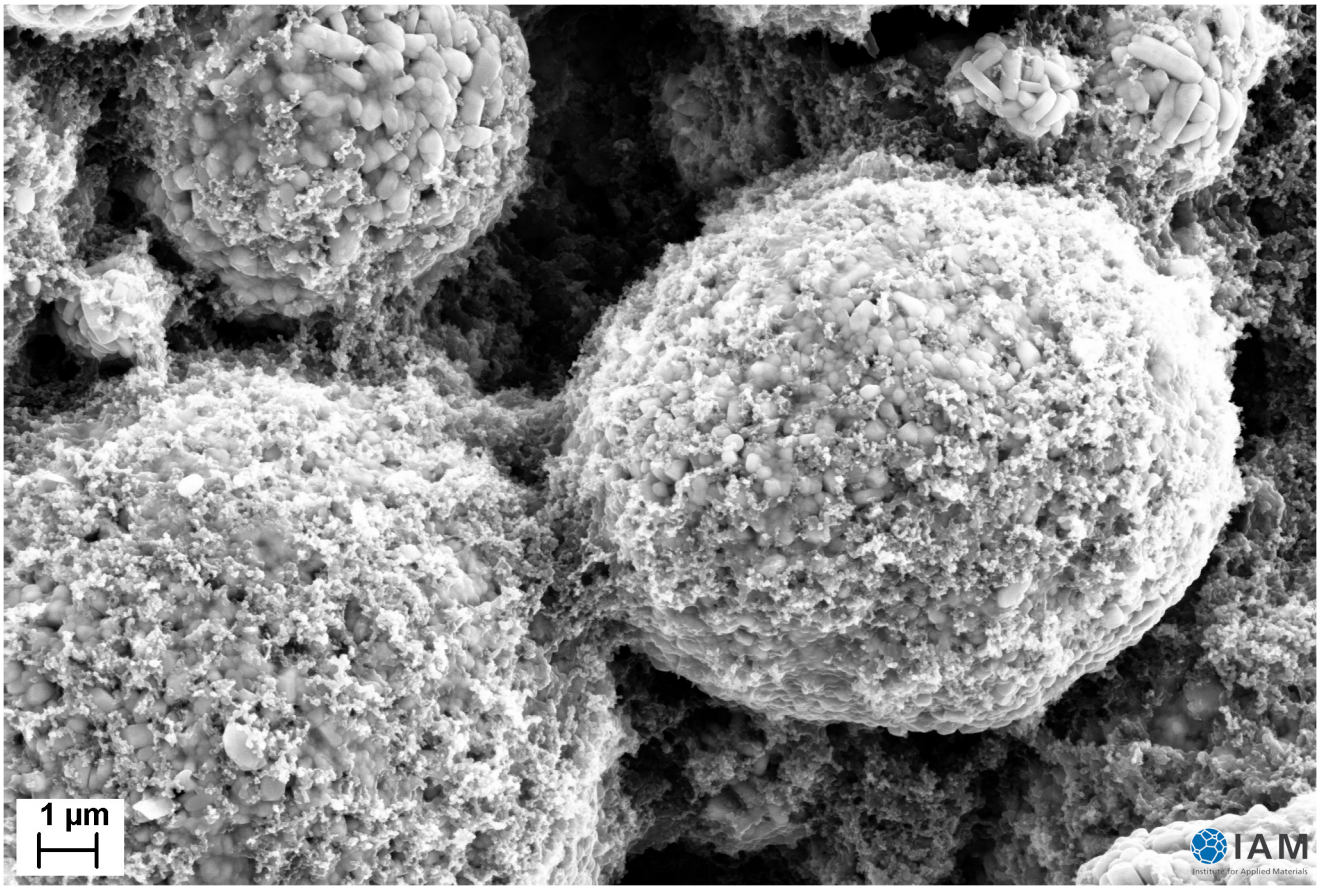

Fig. 4. SEM micrograph of the NMC electrode with homogeneously distributes CB fragments (cast from HAc treated slurry with pH 7).

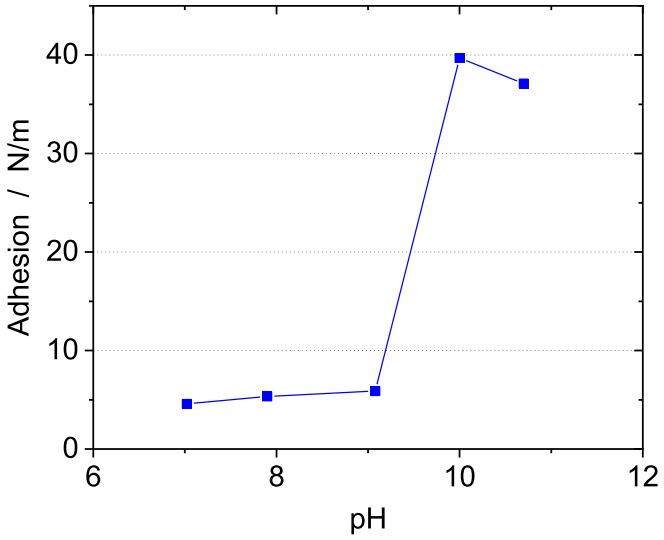

Fig. 5. pH dependence of adhesion strength after the addition of acetic acid.

specific to acetic acid, since the result can also be obtained with many other acids, when the slurry pH is lowered to the range of 8–9 (Fig. 6). However, adhesion failure is primarily not an outcome of the pH value. The reason for the loss of adhesion is more a consequence of the small molecular size of typical inorganic acids. This can be demonstrated by the usage of different PAA grades. While PAA with a molar mass of 2000 g/mol (PAA-2K) negatively affects the adhesion strength, for a high molar mass of 450,000 g/mol (PAA-450K) or 1,250,000 g/mol (PAA-1.25M), the adhesion is even somewhat higher than for the untreated sample. Compared to the larger PAA types, the chain length for PAA-2K is more than 200 times or 600 times shorter. PAA-2K has a molecule size, which is more similar to the other acid examples. By that, it has more the functionality of a dispersant, while the long PAA grades also act like binder molecules.

Adhesion forces between the aluminum, more precisely said, the oxide layer on the aluminum surface and the polymer binder can consist of Van-der-Waals forces, electrostatic forces, acid-base interactions (including H-bonds) [37] or chemical reaction bonds [9]. For the adhesion of most organic polymers, polar attractions based on Lewis acid-Lewis base interactions are important. In aqueous solution, the aluminum oxide surface is amphoteric with both basic and acidic sites [38], forming acid/base bonds with electron accepting or donating sites of the polymer. Oxonium ions and anions from the dissociated acids are also strong Lewis acids/bases. They can migrate to interfaces and replace existing interactions, which hold the molecule to the surface such that the attractions, necessary for adhesion, no longer occur. However, since CMC and the acrylic latex binder are charged polyelectrolytes, their adhesion behavior is also influenced by electrostatic forces. For alumina, usually an isoelectric point (IEP) at a pH of 9.5 is documented [37], although the value may change for different slurry formulations. Below the IEP, the surface has a positive charge, while at higher pH values it is negatively charged. This effect should be responsible for the massive decline of the adhesion strength in this pH region. It is also consistent with the acid/base considerations, as below pH 9, the positively charged surface sites of the alumina, which are also a Lewis acid, favor adsorption of the acetic anion, a strong Lewis base. This concurrent interaction replaces the bonds to the polymeric binder and causes the loss of adhesion (Fig. 7).

Interruption of the original binder bonding is also affected, when PAA is added. However, while the small PAA-2K molecule adheres as a thin layer on the alumina preventing straight interaction with the functional binder groups, the extend PAA-450K or PAA-1.25M molecules adsorb only incompletely on the alumina surface. Parts of the polymer chain form loops and tails that protrude from the surface. This enables diffusion bonding by creating an interdiffusion layer, which consists of the protruding PAA molecules and the polymer chains of the binder (Fig. 8) [39].

Note that the resulting adhesion strength depends on a variety of preparation and environmental factors. For example, adhesion-attenuating effects not always become apparent during a batch preparation of electrodes in laboratories, where typically slow drying processes are applied, while in the convection dryer of this study the evaporation rate of water is much higher. By slow drying at ambient conditions, the adhesion strength of acidic and

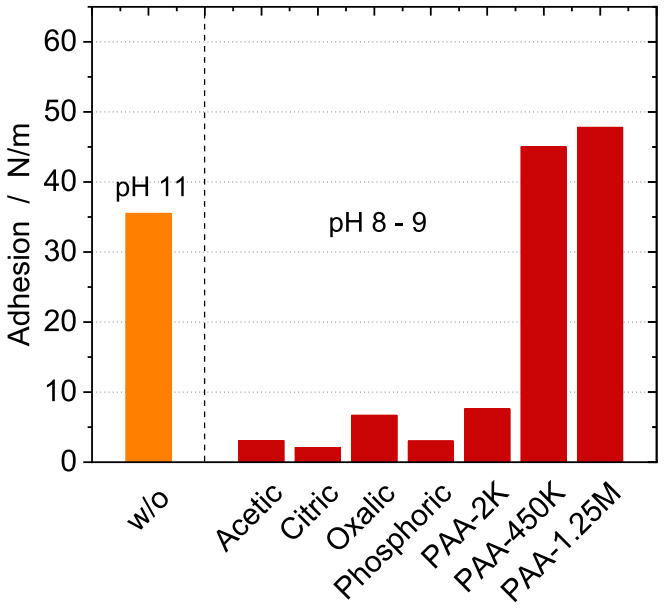

Fig. 6. pH dependence of adhesion strength of NMC electrodes on alumina foil prepared from acid treated slurries with pH 8-9.

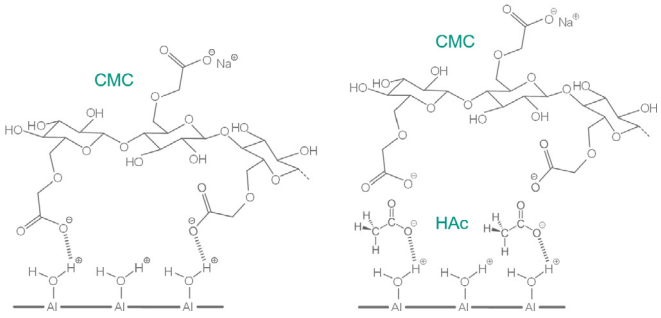

Fig. 7. Adhesive bonds with alumina at pH < IEP. Left: CMC, right: CMC + HAc.

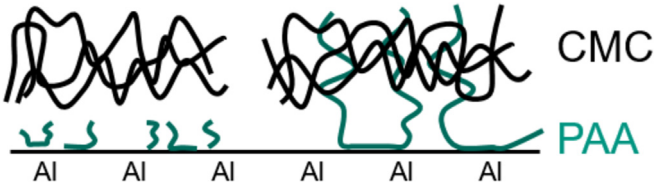

Fig. 8. Formation of diffusion bonding by long-chained PAA molecules.

phosphoric acid treated samples is enhanced significantly at pH 9. The adhesion strength also depends on the volatility of the additives. PAA as a solid, for example, does not evaporate during drying. The remaining amount is therefore independent on drying conditions and ambient conditions. On the other hand, the behavior of the volatile acetic acid is complex. Here, a fast drying process at enhanced temperature can increase the adhesion strength, overcompensating even the negative impact of a higher binder migration [40]. Storage time and ambient conditions are further factors that influence the adhesion strength for acetic acid. All these aspects exceed the scope of the current article. Therefore, they will be taken up in detail in a subsequent paper.

It will be completed that the loss of adhesion is not only attributed to acidic additives. It is a typical problem of small amphiphilic molecules like surfactants or fatty acids, if admixed to the slurry. Due to their polar properties, even uncharged substances concentrate at the bonding interphase and form a so-called weak boundary layer [41]. Examples are dispersants, which are sometimes added in order to improve the carbon black dispersion or to modify the rheological properties of the slurry. A glance at the journals shows that once the electrode adhesion is referred to, usually a low adhesion strength is described after the addition of such molecules [11,42–45]. This leads to the rule of thumb that for reasons of good adhesion, small molecules with molar mass of less than a few hundred thousand g/mol should be avoided as additives in the electrode slurry.

3.4. Electrochemical behavior of acid modified electrodes

The acetic acid treated electrodes show minor differences during the formation cycles at C/20. An expected theoretical capacity of 155 mAh/g is not yielded completely. The average capacity loss due to the hydrolysis of the NMC is in the range of 3%–7% (Fig. 9). With increasing C rate a more pronounced dependency of the specific capacity on the pH of the slurry becomes obvious, with a maximum at pH 9 (Fig. 9 insert). This result correlates with the increasing cell impedance at low pH values, but does not reflect the low impedance for a pH above 9 (Fig. 3).

It is assumed that additional features of the electrode structure influence the charge transport. Besides good electrical conductivity, also fast ionic transport is a prerequisite for powerful electrodes. Apparently, carbon black agglomerates and carbon-binder-domains within the pores impede the overall ion transport in the electrode due to the less favorable tortuosity [46,47]. The high dispersing potential of the acid gives rise to a reduction of the number and the size of the carbon black agglomerates. Initially, this

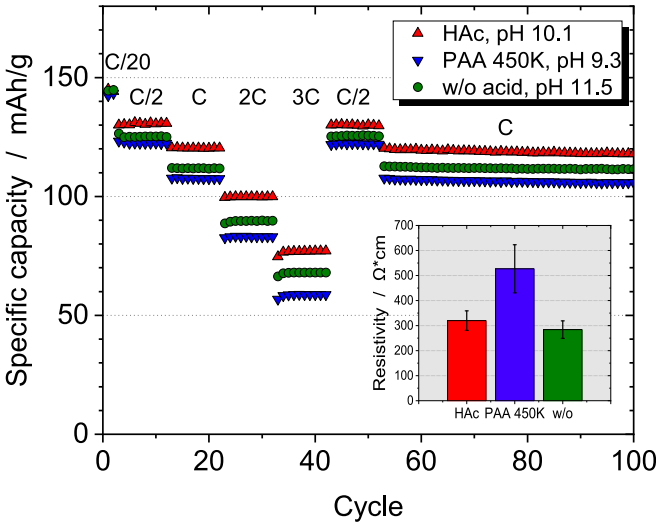

Fig. 10. Rate capability tests of NMC-graphite cells after slurry treatment with acetic acid and PAA-450K, supplemented by a cell without slurry modification. The insert shows the respective resistivity of the cathodes.

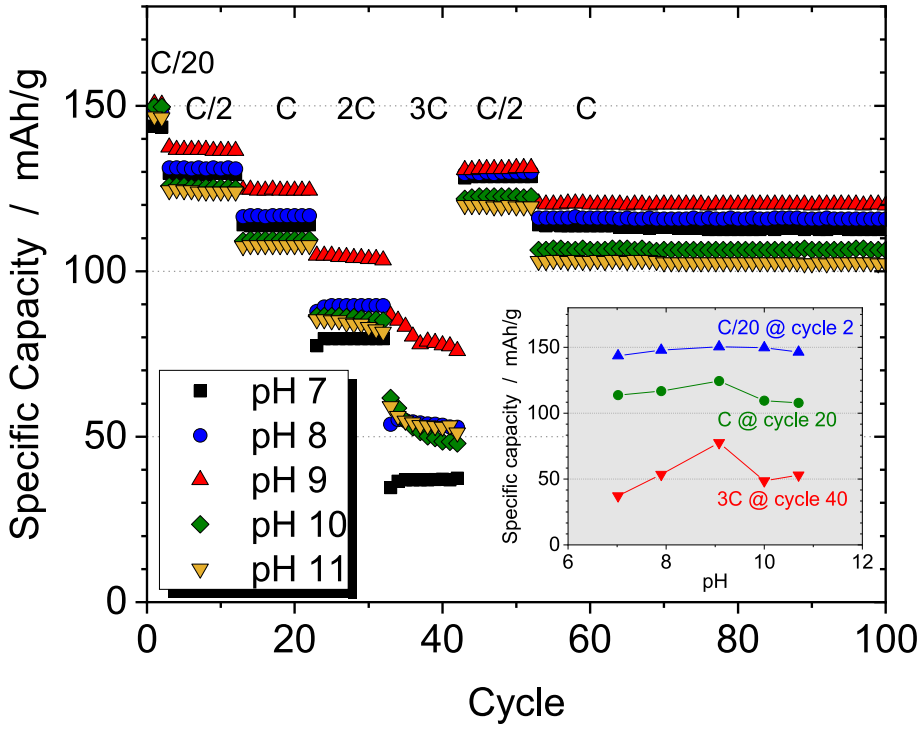

Fig. 9. Rate capability of NMC-graphite cells with slurry pH control by acetic acid.

enables a more efficient ion transport through the electrolyte by reducing the electrode tortuosity. Below pH 9 the overvoltage due to the reduction of the electronic conductivity becomes the limiting factor, which is responsible for the decline of the specific capacity, expressed especially for the high C rate cycles.

The cycle aging behavior was tested with cells prepared from slurries containing acetic acid or PAA-450K as pH modifier. Although the electrode without acid addition is clearly foamed, compaction by calendaring allowed the preparation of cells for comparison. Fig. 10 shows the results of the initial CC segment. It can be seen that, except for the formation cycles at C/20, significantly higher capacities are obtained with acetic acid, while the performance with PAA is even lower than for the acid-free cell. The later result is caused by the overpotential due to a higher resistivity of PAA containing electrodes (Fig. 10 insert). Since the acetic acid sample has a resistivity comparable to that of the acid-free sample, this cannot be an explanation for the improved rate capability. Here, also a more efficient ion transport by a reduced electrode tortuosity is conceivable, but requires further investigations.

Following the initial CC segment, the test procedure was continued in CCCV mode at 2C/3C, interrupted by a 10-cycle segment with 1C charging/discharging rate after each 100 CCCV cycles. This stage starts with the same succession as in the CC run. The slurry, which was modified with acetic acid, initially receives the highest capacities, whereas with PAA the capacity is the lowest. Then, the acetic acid sample suffers a more expressed degradation leading to the lowest capacity values after 600 cycles (Fig. 11). Interestingly, the cell without acid addition reveals the lowest degradation. After 400 cycles, it dominates all other samples. It is very likely that the stronger degradation is affected by the acid. The decline of the acetic acid sample is therefore an indication that despite of its high volatility, acetic acid residues must have remained in the electrode layer, withstanding even the drying steps after coating and before cell assembling. The cell with PAA shows only a moderately stronger degradation as the acid-free cell. This might be caused by the diffusion bonding of the PAA in the interface, which prevents a quick dissolution in the electrolyte.

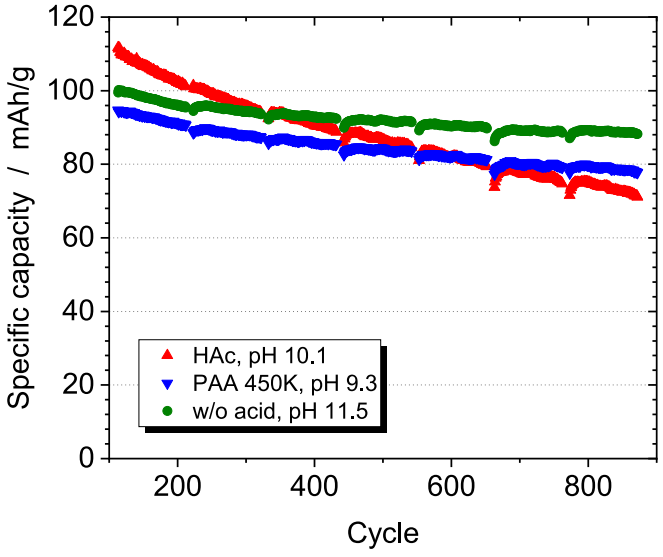

Fig. 11. Aging tests at 2C/3C using the samples from Fig. 10. After each 100 CCCV cycles, the run was interrupted by a 10 cycle CC segment at 1C (not shown for reasons of clarity).

Post-mortem investigations of the electrodes can give a hint on the nature of the acid attack. Cross sections of the electrodes after 900 cycles reveal that for acid modified samples, the NMC particles show an increased number of internal cracks (Fig. 12). These cracks would explain the capacity decline in the CCCV cycles as they act as barriers for the diffusion of the lithium ions and in some cases even the isolation of regions is possible, which will reduce the capacity determining NMC quantity. Nevertheless, a disclosure of the underlying processes is still pending.

4. Summary

The water sensitivity of cathode materials is a serious obstacle to the industrial acceptance of an aqueous processing route. In contact with water, lithium ions are leached out of the material, generating a noticeable loss of capacity due to the formation of lithium hydroxide and insoluble carbonates. The increase of the slurry pH is a secondary effect, which affects the coating process, since a high pH value leads to corrosive attack of the aluminum current collector film with negative consequences on electrode homogeneity and cell properties.

An obvious approach to avoid or to diminish the corrosion of the aluminum is to lower the pH by the addition of an acid to the slurry. However, this measure has consequences for the processing of the slurry and the properties of the cells made therefrom. This was demonstrated exemplarily for acetic acid as pH modifier. For a complete suppression of the corrosive attack, the pH must be

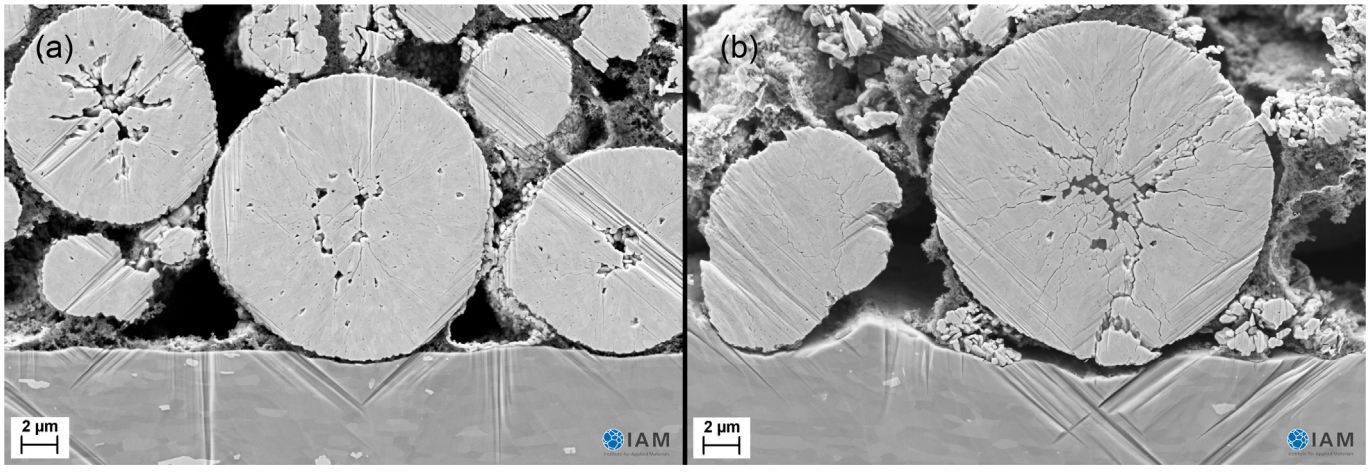

Fig. 12. Post-mortem SEM micrographs of NMC particles after 900 cycles, without (left) and with addition of acetic acid to the slurry (right).

reduced beneath a pH of 8.5. Unfortunately, significant leaching of cations from the cathode material already takes place at this pH value. Additionally, the viscosity of the slurry and the resistance of the electrode is rising, while the adhesion of the cathode layer to the current collector is strongly reduced. The rise of viscosity and resistance is presumably caused by the high dispersing potential of the acid creating more isolated carbon black fragments, while an accumulation of acid in the adhesion-determining interphase is responsible for the adhesion drop. By a moderate acid addition to the pH range of 9–10, alumina corrosion can only be avoided incompletely. However, this region seems to represent an optimum pH range for the electrode and cell properties. The unfavorable pH effects are not limited to acetic acid. In particular, the negative effect on the adhesion strength is common to most acids, as well as to other polar additives. Only organic acids with very high molecular weight, e.g. PAA, do not suffer this adhesion problem, as their extended polymer chains enable a supporting diffusion bonding. Another outcome, which is caused by the addition of acetic acid, is an increased cell degradation. Although the reason is not known yet, post mortem studies of aged cells indicate that damage of the cathode material by cracks seems to be responsible for it.

In the light of these findings, it is recommended to make sure that first the primary interaction between water is suppressed or at least reduced, since it also prevents the secondary formation of alumina corrosion. A promising method is the coating of the particles ("artificial SEI"). In this case, one has to balance between a complete, but possibly charge-transfer impeding, coating and a thin but not completely covering layer. For high-capacity materials, the application of a two-step approach - reduction of lithium leaching by a thin coating and subsequent handling the remaining corrosion by moderate pH modification - could be a feasible strategy. The investigation of the acid impact, especially in order to control the aging behavior, therefore continues to be significant for aqueous processing.

Acknowledgment

The authors gratefully acknowledge delivery of the NMC material by BASF and the support of the Chemical Analysis Group of Thomas Bergfeldt (IAM-AWP) by performing the ICP-OES measurements. This work contributes to the research performed at CELEST (Center for Electrochemical Energy Storage Ulm-Karlsruhe).

References

[1] J. Li, C. Daniel, D. Wood, J. Power Sources 196 (2011) 2452–2460. https://doi.org/10.1016/j.jpowsour.2010.11.001.
[2] Z. Zhang, T. Zeng, Y. Lai, M. Jia, J. Li, J. Power Sources 247 (2014) 1–8. https://doi.org/10.1016/j.jpowsour.2013.08.051.
[3] S.F. Lux, F. Schappacher, A. Balducci, S. Passerini, M. Winter, J. Electrochem. Soc. 157 (2010) A320–A325. https://doi.org/10.1149/1.3291976.
[4] L. Jabbour, R. Bongiovanni, D. Chaussy, C. Gerbaldi, D. Beneventi, Cellulose 20 (2013) 1523–1545. https://doi.org/10.1007/s10570-013-9973-8.
[5] A. Moretti, G.-T. Kim, D. Bresser, K. Renger, E. Paillard, R. Marassi, M. Winter, S. Passerini, J. Power Sources 221 (2013) 419–426. https://doi.org/10.1016/j.jpowsour.2012.07.142.
[6] D.L. Wood, J. Li, C. Daniel, J. Power Sources 275 (2015) 234–242. https://doi.org/10.1016/j.jpowsour.2014.11.019.
[7] S. Ahmed, P.A. Nelson, K.G. Gallagher, D.W. Dees, J. Power Sources 322 (2016) 169–178. https://doi.org/10.1016/j.jpowsour.2016.04.102.
[8] B. Lestriez, Compt. Rendus Chem. 13 (2010) 1341–1350. https://doi.org/10.1016/j.crci.2010.01.018.
[9] N.S. Hochgatterer, M.R. Schweiger, S. Koller, P.R. Raimann, T. Wöhrle, C. Wurm, M. Winter, Electrochem. Solid State Lett. 11 (2008) A76–A80. https://doi.org/10.1149/1.2888173.
[10] J. Xu, S.-L. Chou, Q.-f. Gu, H.-K. Liu, S.-X. Dou, J. Power Sources 225 (2013) 172–178. https://doi.org/10.1016/j.jpowsour.2012.10.033.
[11] C.-C. Li, J.-T. Lee, X.-W. Peng, J. Electrochem. Soc. 153 (2006) A809–A815. https://doi.org/10.1149/1.2177071.
[12] I. Doberdò, N. Löffler, N. Laszczynski, D. Cericola, N. Penazzi, S. Bodoardo, G.-T. Kim, S. Passerini, J. Power Sources 248 (2014) 1000–1006. https://doi.org/10.1016/j.jpowsour.2013.10.039.
[13] I.A. Shkrob, J.A. Gilbert, P.J. Phillips, R. Klie, R.T. Haasch, J. Bareño, D.P. Abraham, J. Electrochem. Soc. 164 (2017) A1489–A1498. https://doi.org/10.1149/2.0861707jes.
[14] G.V. Zhuang, G. Chen, J. Shim, X. Song, P.N. Ross, T.J. Richardson, J. Power Sources 134 (2004) 293–297. https://doi.org/10.1016/j.jpowsour.2004.02.030.
[15] X. Zhang, W.J. Jiang, X.P. Zhu, A. Mauger, Qilu, C.M. Julien, J. Power Sources 196 (2011) 5102–5108. https://doi.org/10.1016/j.jpowsour.2011.02.009.
[16] J. Kim, Y. Hong, K.S. Ryu, M.G. Kim, J. Cho, Electrochem. Solid State Lett. 9 (2006) A19–A23.
[17] R. Jung, R. Morasch, P. Karayaylali, K. Phillips, F. Maglia, C. Stinner, Y. Shao-Horn, H.A. Gasteiger, J. Electrochem. Soc. 165 (2018) A132–A141. https://doi.org/10.1149/2.0401802jes.
[18] W. Porcher, P. Moreau, B. Lestriez, S. Jouanneau, D. Guyomard, Electrochem. Solid State Lett. 11 (2008) A4–A8.
[19] C.-C. Li, J.-T. Lee, Y.-L. Tung, C.-R. Yang, J. Mater. Sci. 42 (2007) 5773–5777. https://doi.org/10.1007/s10853-006-1172-7.
[20] B.C. Church, D.T. Kaminski, J. Jiang, J. Mater. Sci. 49 (2014) 3234–3241. https://doi.org/10.1007/s10853-014-8028-3.
[21] K. Kimura, T. Sakamoto, T. Mukai, Y. Ikeuchi, N. Yamashita, K. Onishi, K. Asami, M. Yanagida, J. Electrochem. Soc. 165 (2018) A16–A20. https://doi.org/10.1149/2.0241802jes.
[22] X. Xiong, Z. Wang, P. Yue, H. Guo, F. Wu, J. Wang, X. Li, J. Power Sources 222 (2013) 318–325. https://doi.org/10.1016/j.jpowsour.2012.08.029.
[23] D. Carvalho, N. Loeffler, G.-T. Kim, M. Marinaro, M. Wohlfahrt-Mehrens, S. Passerini, Polymers 8 (2016) 276. https://doi.org/10.3390/polym8080276.
[24] M. Kuenzel, D. Bresser, T. Diemant, D.V. Carvalho, G.-T. Kim, R.J. Behm, S. Passerini, ChemSusChem 11 (2018) 562–573. https://doi.org/10.1002/cssc.201702021.
[25] M. Memm, A. Hoffmann, M. Wohlfahrt-Mehrens, Electrochim. Acta 260 (2018) 664–673. https://doi.org/10.1016/j.electacta.2017.12.014.
[26] G.T. Kim, S.S. Jeong, M. Joost, E. Rocca, M. Winter, S. Passerini, A. Balducci, J. Power Sources 196 (2011) 2187–2194. https://doi.org/10.1016/j.jpowsour.2010.09.080.
[27] N. Loeffler, G.-T. Kim, F. Mueller, T. Diemant, J.-K. Kim, R.J. Behm, S. Passerini, ChemSusChem 9 (2016) 1112–1117. https://doi.org/10.1002/cssc.201600353.
[28] N. Loeffler, J. von Zamory, N. Laszczynski, I. Doberdo, G.-T. Kim, S. Passerini, J. Power Sources 248 (2014) 915–922. https://doi.org/10.1016/j.jpowsour.2013.10.018.
[29] N. Laszczynski, J. von Zamory, J. Kalhoff, N. Loeffler, V.S.K. Chakravadhanula, S. Passerini, ChemElectroChem 2 (2015) 1768–1773. https://doi.org/10.1002/celc.201500219.
[30] Z. Wang, N. Dupré, A.-C. Gaillot, B. Lestriez, J.-F. Martin, L. Daniel, S. Patoux, D. Guyomard, Electrochim. Acta 62 (2012) 77–83. https://doi.org/10.1016/j.electacta.2011.11.094.
[31] C.-C. Li, Y.-S. Lin, J. Power Sources 220 (2012) 413–421. https://doi.org/10.1016/j.jpowsour.2012.07.125.
[32] F.A. Çetinel, W. Bauer, Bull. Mater. Sci. 37 (2014) 1685–1690. https://doi.org/10.1007/s12034-014-0733-7.
[33] U. Kaestner, H. Hoffmann, R. Doenges, J. Hilbig, Colloids Surface. 123–124 (1997) 307–328.
[34] F.H. Chowdhury, S.M. Neale, J. Polym. Sci. Part A 1 (1963) 2881–2891.
[35] J.-H. Lee, S. Lee, U. Paik, Y.-M. Choi, J. Power Sources 147 (2005) 249–255. https://doi.org/10.1016/j.jpowsour.2005.01.022.
[36] K. Kuratani, K. Ishibashi, Y. Komoda, R. Hidema, H. Suzuki, H. Kobayashi, J. Electrochem. Soc. 166 (2019) A501–A506. https://doi.org/10.1149/2.0111904jes.
[37] E. McCafferty, J. Electrochem. Soc. 150 (2003) B342. https://doi.org/10.1149/1.1580135.
[38] J. Mattisson, The Influence of Carboxylic Acid in Packaging Materials, Lund University, 2016.
[39] S.S. Voyutskii, V.L. Vakula, J. Appl. Polym. Sci. 7 (1963) 475–491. https://doi.org/10.1002/app.1963.070070207.
[40] S. Jaiser, M. Müller, M. Baunach, W. Bauer, P. Scharfer, W. Schabel, J. Power Sources 318 (2016) 210–219. https://doi.org/10.1016/j.jpowsour.2016.04.018.
[41] J.J. Bikerman, Industrial and Enginering Chemistry 59 (1967) 40–44.
[42] C.-C. Li, J.-T. Lee, C.-Y. Lo, M.-S. Wu, Electrochem. Solid State Lett. 8 (2005) A509. https://doi.org/10.1149/1.2012287.
[43] W. Porcher, B. Lestriez, S. Jouanneau, D. Guyomard, J. Electrochem. Soc. 156 (2009) A133–A144.
[44] W. Porcher, B. Lestriez, S. Jouanneau, D. Guyomard, J. Power Sources 195 (2010) 2835–2843. https://doi.org/10.1016/j.jpowsour.2009.11.088.
[45] B. Bitsch, J. Dittmann, M. Schmitt, P. Scharfer, W. Schabel, N. Willenbacher, J. Power Sources 265 (2014) 81–90. https://doi.org/10.1016/j.jpowsour.2014.04.115.
[46] S. Vierrath, L. Zielke, R. Moroni, A. Mondon, D.R. Wheeler, R. Zengerle, S. Thiele, Electrochem. Commun. 60 (2015) 176–179. https://doi.org/10.1016/j.elecom.2015.09.010.
[47] D.E. Stephenson, B.C. Walker, C.B. Skelton, E.P. Gorzkowski, D.J. Rowenhorst, D.R. Wheeler, J. Electrochem. Soc. 158 (2011) A781–A789.